Sedov Blast Wave Propagation

ASTRON 255 PROJECT III

Blake Drechsler
Ruoyi Yin

March 25, 2020

1 Introduction

This project is about simulating Sedov Blast Wave propagation using finite difference method. The partial differential equations can be represented by finite difference equations and thus calculations can be carried out by computer programming. For this project specifically, we evaluate the propagation of 1-D Blast wave. Even though the blast wave propagation is in 3 dimensions, we can model it as in 1-D since the propagation is isotropic. In this report, the numerical solutions of Sedov Blast Wave are shown, semi-analytical solutions are presented and the comparison between numerical solutions and semi-analytical solutions are demonstrated. In the second section, we provide methods and initial conditions used in numerical simulations. In the third section, results and plots are shown. In the Fourth section, we discuss and compare numerical with semi-analytical solutions and answer the questions listed in lecture notes.

2 Methods

2.1 Finite Difference Method

We use Python to run blast wave propagation. Since the wave evolves with time, we construct two loops, one of them loops through time, and in each time-step we also loop through each spatial step.

Our independent variable is time, dependent variables are coordinate (x), velocity (u), energy (E), pressure (P), density (ρ) and artificial viscosity (q). Specifically, x is defined at integer time and integer space points; u is defined at half-integer time and integer space; E, P, and ρ are defined at integer time and half-integer space; q is defined at half-integer time and half-integer space.

For boundary & initial conditions: x and u are specified from spatial step 0 to 130 (131 points). E, P, q and ρ are specified at 0.5 - 129.5 (130 points). Additionally, P and q are also defined at inner boundary. The P value at inner boundary is set to be $1.33 * 10^5$, the q value at inner boundary is 0. For the first 5 spatial zones in the first time step, we assign specific internal energy to be 10^{10} in order to simulate the release of energy initially that drives blast wave propagation.

In the simulation, we apply equal radial zoning, so Δm is different at each spatial step, so we define an initial Δm for each spatial interval. The Δt is set to be $1 * 10^{-6}$.

At each time-step, we utilize 6 equations to update 6 variables respectively. First, we update velocity, then position, density, artificial viscosity, energy, and at last pressure. The detailed equations and steps are shown in Lecture Note P.96-97. Besides, the first three equations are modified to fit the spherical shape of blast wave propagation (Lecture Note P.112).

2.2 Artificial Viscosity

We include both linear and quadratic terms of artificial viscosity. C_0^2 is the coefficient for quadratic q term, and C_1 is the coefficient for linear q term. The value we used for C_0^2 is 1 for C_1 is 0.5.

3 Results

Figure 1 displays the pressure, artificial viscosity, density and velocity versus position plots when the wave front propagates to around r = 100 (based on the peak on artificial viscosity plot). Since we set the time step to be 10^{-6} and loops through 40000 times, the Δt after the initial energy release is t = 0.04.

4 Discussion

In this section, we will address the 4 questions listed in lecture notes for this project and talk about glitches separately.

4.1 Comparison with Similarity Variables

Here we answer the first question in lecture note P.120.

The equations for similarity variables are:

$$P = \frac{D^2 \rho_0}{\gamma} f \tag{1}$$

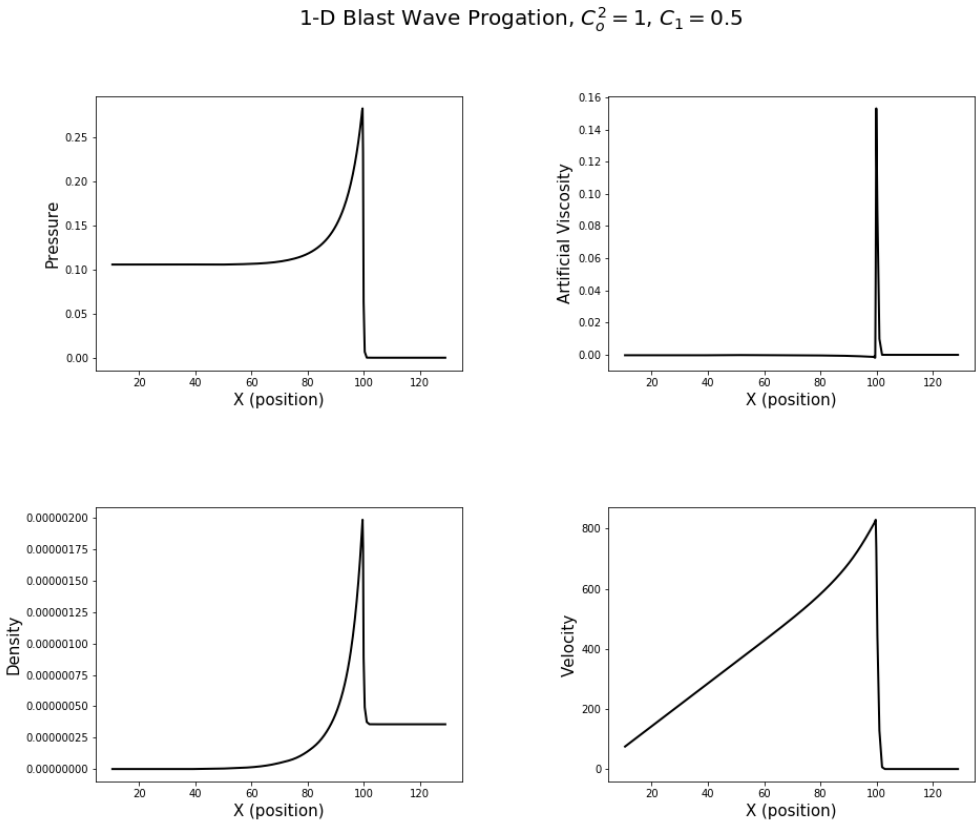

Figure 1: Blast wave propagation for $C_0^2 = 1$ and $C_1 = 0.5$, when R = 100, t = 0.04. Four plots are pressure, artificial viscosity, density, and velocity versus coordinate position respectively (Numerical Solutions).

$$u = D\phi \tag{2}$$

$$\frac{\rho}{\rho_0} = \psi \tag{3}$$

where f, ϕ, and ψ are 3 similarity variables for pressure, velocity and density respectively. P_0, ρ_0 are initial conditions for pressure and density in the outside medium. D is the shock velocity. Using these 3 equations, we can re-scale our original pressure, velocity and density functions to the similarity variables that can be used to compare with results in Taylor's paper [3]. Then, by also re-scaling position variable to $\eta = r/R(t)$, we are able to extract both numerical and self-similar solutions at several different η values and then compare the results quantitatively.

However, in order to do the comparison, we need to also get D for the numerical solution. Therefore, we utilize the equation:

$$D = \frac{\partial R}{\partial t} = \frac{2}{5}\frac{R(t)}{t} \tag{4}$$

where after calculation we get the D value to be 1000.

At R = 100, the shock velocity is 1000 and our initial conditions include: γ = 1.4, $\rho_0 = 3.57 * 10^{-7}$, $P_0 = 1.33 * 10^5$, $u_0 = 0$, and specific energy at first 5 spatial zones are $e = 10^{10}$. The results are shown in Table 1:

Table 1: A Table Comparing Semi-Analytical Solutions & Numerical Solutions.

Entries	η **= 0.5**	η **= 0.6**	η **= 0.8**	η **= 0.9**	η **= 1**
f^*	0.415	0.418	0.462	0.584	1.111
ϕ^*	0.358	0.425	0.580	0.682	0.825
ψ^*	0.013	0.040	0.386	1.216	5.565
f	0.436	0.438	0.478	0.593	1.167
ϕ	0.375	0.443	0.590	0.687	0.833
ψ	0.007	0.034	0.370	1.177	6.000

f^*, ϕ^*, and ψ^* represent similarity variable values calculated from numerical solutions by finding the point closest to the 5 different η values, while the last 3 similarity values represent results from Taylor's calculation [3].

4.1.1 Similarity Variables vs. η

Taylor only expresses the similarity variables depend on η with derivative terms, but does not do the integral explicitly. Landau solves the exact solutions including 3 similarity variables and η [2]:

$$f = \frac{\gamma(\gamma-1)(1-\phi)\phi^2}{2(\gamma\phi-1)} \tag{5}$$

$$\eta^5 = [\frac{1}{2}(\gamma+\phi]^{-2}\left\{\frac{\gamma+1}{7-\gamma}[5-(3\gamma-1)\phi]\right\}^{v_1}\left[\frac{\gamma+1}{\gamma-1}(\gamma\phi-1)\right]^{v_2} \tag{6}$$

$$\psi = \frac{\gamma+1}{\gamma-1}\left[\frac{\gamma+1}{\gamma-1}(\gamma\phi-1)\right]^{v_3}\left\{\frac{\gamma+1}{7-\gamma}[5-(3\gamma-1)\phi]\right\}^{v_4}\left[\frac{\gamma+1}{\gamma-1}(1-\phi)\right]^{v_5} \tag{7}$$

$$v_1 = -\frac{13\gamma^2-7\gamma+12}{(3\gamma-1)(2\gamma+1)} \tag{8}$$

$$v_2 = \frac{5(\gamma-1)}{2\gamma+1} \tag{9}$$

$$v_3 = \frac{3}{2\gamma+1} \tag{10}$$

$$v_4 = -\frac{v_1}{2-\gamma} \tag{11}$$

$$v_5 = -\frac{2}{2-\gamma} \tag{12}$$

4.2 Further Comparison and Thickness Analysis

Here we address the second question in the lecture note P.120.

In order to compare the numerical solutions with the expected behavior of f, ϕ, and ψ, we plot the results together.

First, for f, we focus on the near constancy behavior of f, which is the asymptotic value of f as η decreases and approaches to 0. In Taylor's paper, the asymptotic value is specified as $f = 0.436$ [3]. Figure 2 shows that the as

η approaches 0, the f value from calculation approaches the asymptotic value 0.436 (yellow curve), in the same plot, we also show the curve from Taylor's calculation for f for better comparison (red curve). The numerical solutions are lined up with both the asymptotic value and step-by-step calculation from Taylor [3].

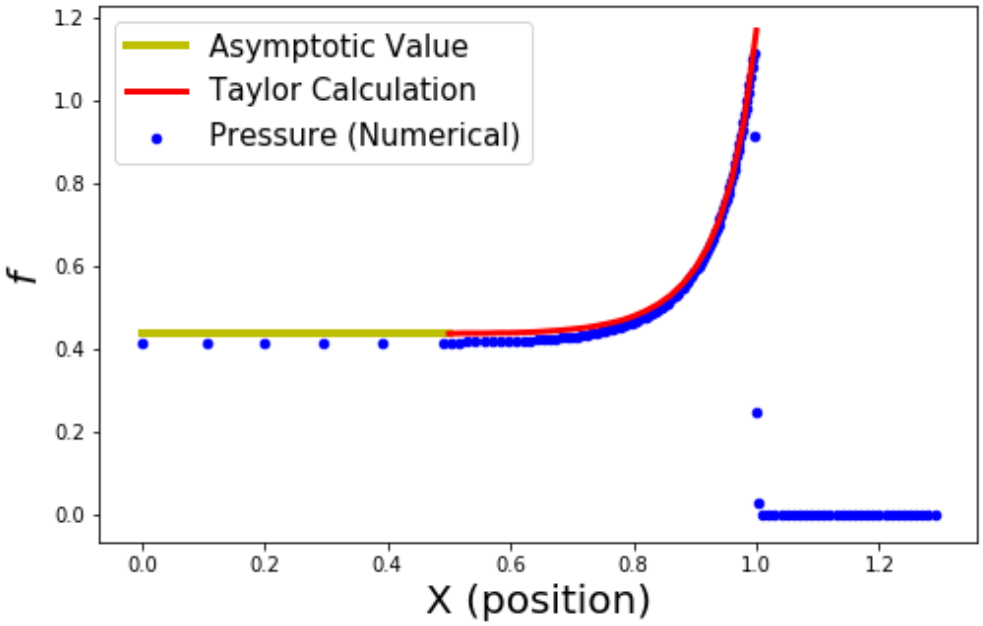

Figure 2: Comparison between numerically-calculated f and Taylor's result. Yellow curve shows the asymptotic f value as η approaches 0. Red curve shows Taylor's step-by-step calculation result.

Second, we want to compare the numerical results with the expected behavior of ϕ extrapolated to origin. In Taylor's paper, as η approaches 0, ϕ is linearly related to η based on the equation $\phi = \eta/\gamma$ [3]. Figure 3 demonstrates this linear trend (yellow curve), the Taylor step-by-step calculation results are also shown for comparison (red curve). The numerical solutions are lined up with both the linear trend and the step-by-step calculation from Taylor [3].

Third, we want to compare the drop-off behavior of ψ in the numerical solution to Taylor's step-by-step calculation and approximate formulae. Taylor demonstrates that when η is small, the formula for ψ approaches [3]:

$$\psi = D\eta^{3/(\gamma-1)} \tag{13}$$

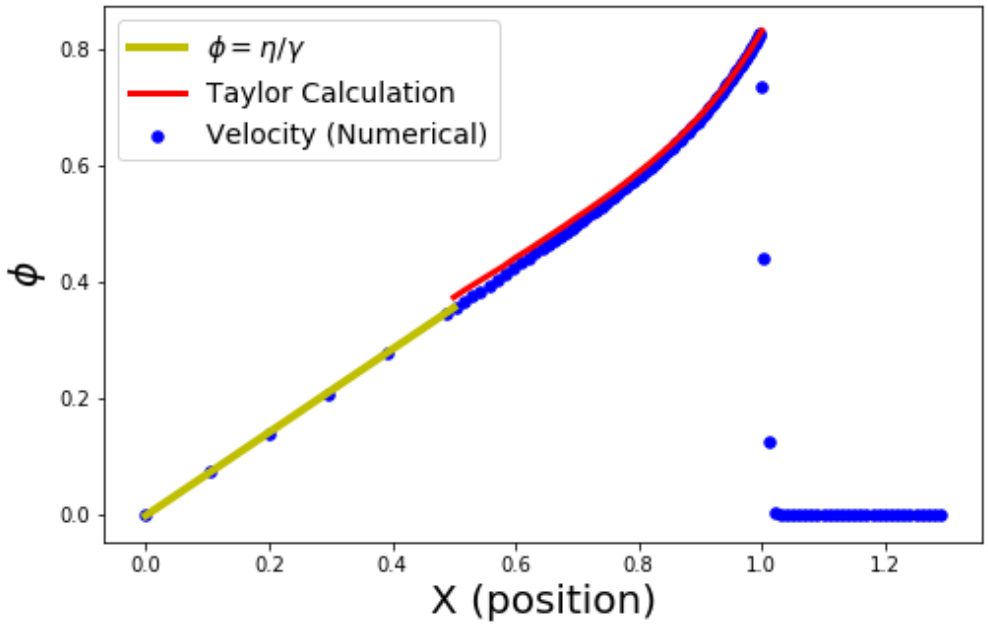

Figure 3: Comparison between numerically-calculated ϕ and Taylor's result. Yellow curve shows the linear trend of ϕ as η approaches 0 ($\phi = \eta/\gamma$). Red curve shows Taylor's step-by-step calculation result.

Figure 4 demonstrates both the approximate formula (yellow curve), and Taylor step-by-step calculation (red curve). The numerical solutions are lined up with both the approximate formula and the step-by-step calculation from Taylor [3].

4.2.1 Thickness of the Snow-Plowed Layer

In the blast wave propagation, the mass in the original medium would be swept up by the wave, and a dense shell would form at the boundary. When the shock is strong, the conditions in the shock wave follow the jump conditions:

$$\rho_{sh} \approx \frac{\gamma + 1}{\gamma - 1}\rho_0 \tag{14}$$

Since the external medium is uniform, we can calculate the mass contained inside the blast wave shell:

$$M_{sw} = \frac{4\pi}{3}\rho_0 R^3 \tag{15}$$

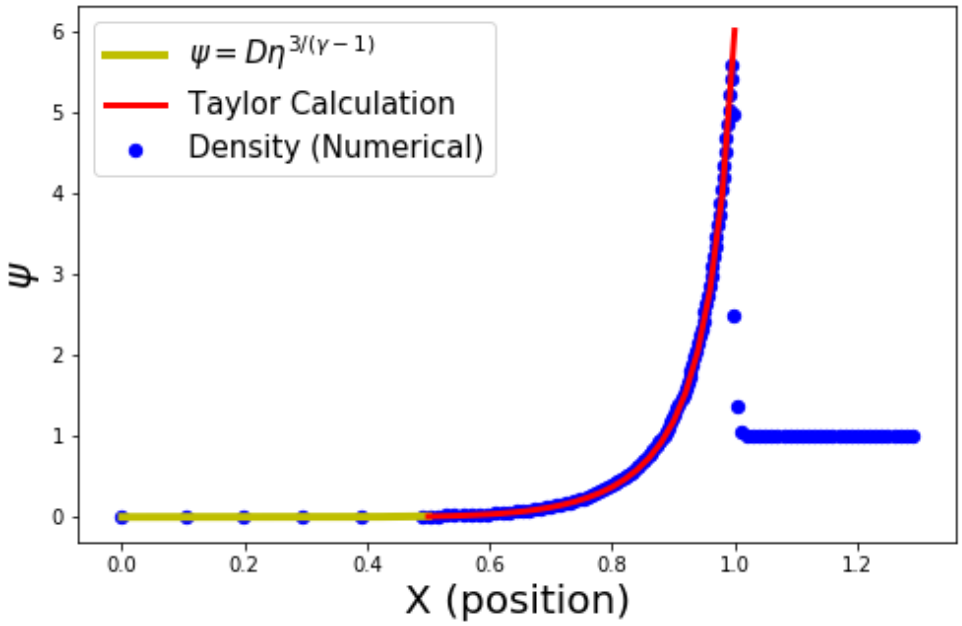

Figure 4: Comparison between numerically-calculated ψ and Taylor's result. Yellow curve shows the approximate formula result of ψ as η approaches 0. Red curve shows Taylor's step-by-step calculation result.

Since the post-shock region has higher density than the pre-shock region, right now most of the mass is piled up in or close to the shock front. Therefore, by using conservation of mass, we can calculate the thickness of the piled-up region (snow-plowed region):

$$M_{sw} \approx 4\pi\rho_{sh}R^2\Delta R \tag{16}$$

Combining equation 14, 15, 16, we can derive the thickness:

$$\Delta R = \frac{(\gamma-1)R}{3(\gamma+1)} = 0.056R \tag{17}$$

Therefore, in our problem, the thickness of the show-plowed layer is 5.6.

Then, we want to determine the thickness of snow-plowed layer in the numerical solution by different metrics.

First, we consider the ψ vs. η plot, since we get the analytical solution for thickness from density difference. We apply the cutoff in the post-shock

region when ρ in the post-shock region approaches that in the pre-shock region. From calculation, the inner cutoff point after calculation is 88.38. Since we choose the outer cutoff point to be 100. The thickness from this metric is 11.62.

Second, we still focus on the ψ vs. η plot. This time we want to find the point in the post-shock region where density drops by a factor of e. After calculation, the inner cutoff point is 93.753, the outer cutoff point is 100, so the thickness is 6.247, closer to the analytical solution.

Third, we consider the ϕ vs. η plot, and try to find the point in the post-shock region where the result starts to deviate from the linear trend by a value larger than 0.05. After calculation, we get the inner cutoff point 91.94, and outer cutoff point is still 100. Therefore, the thickness from this metric is 8.06.

Therefore, within all three metrics that we use to calculate the thickness numerically, the second one returns the result that's closest to the analytical thickness.

4.3 Shock Velocity vs. R(t)

Here we answer question 3 in P.121.

First, we would work out the semi-analytical solution:

$$D = \frac{2R}{5t} = \frac{2}{5}\beta\left(\frac{E}{\rho_0}\right)^{1/5} t^{-3/5} \tag{18}$$

where D is the shock velocity, and β is the constant depends on γ (the full derivation will be discussed in the next subsection for solving question 4).

We choose $D \propto R^{-3/2}$ due to the fact that $D \propto t^{-3/5}$.

Then, we show the equation for R(t):

$$R^{-3/2} = \beta^{-3/2}\left(\frac{E}{\rho_0}\right)^{-3/10} t^{-3/5} \tag{19}$$

By plugging in values, we find that analytically:

$$D = 989938.36 R^{-3/2} \tag{20}$$

Then, we try to find how the shock velocity varies with the position of the front and see how it compares with the analytical solution. To find the relationship between D and R_{shock} in our simulation, we first need to find the shock velocity at various times in the numerical simulation. To do this we plot the artificial viscosity vs. r at different times. We choose to look at this q parameters since it is the clearest way to find the location of the shock front. We examine this quantity at 8 different, equally spaced values for time. Once we have a plot of q vs R we could calculate the shock position by finding the position of the peak. To find this position, we simply take the point, centered on the maximum value of the peak of q. We also use this method to find the position of the shock at times shortly after each of the 8 already mentioned time in order to calculate the velocity. This is shown for 2 of these times in the figure below:

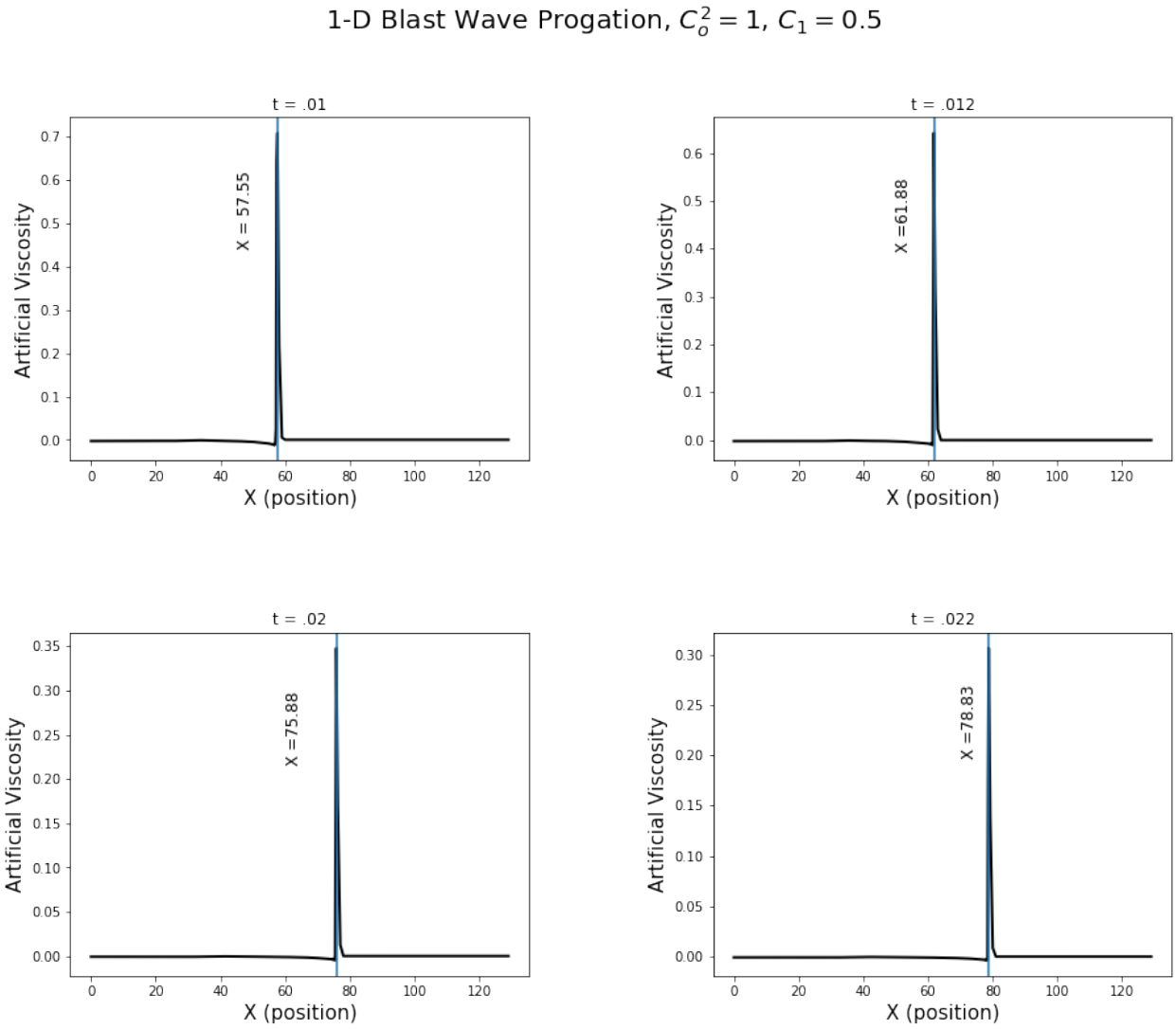

Figure 5: A plot of artificial viscosity vs. position at the times t = 0.01 and t = 0.02 and shortly after those times. The vertical lines denote the centroid of the peaks and their positions have been labeled.

We can estimate the shock velocity at a given time by taking the difference between the shock position at the time and a slightly later time, then dividing by the elapsed time (We used a dt of 0.002). We then use this method to find the shock positions and velocities at 8 different times. We also record where the shock front is at the time by taking the average position of the shock between the time chosen and the time slightly later. Now, we can make a plot of shock velocity vs. shock position and compare it to the semi-analytical solution which is shown below:

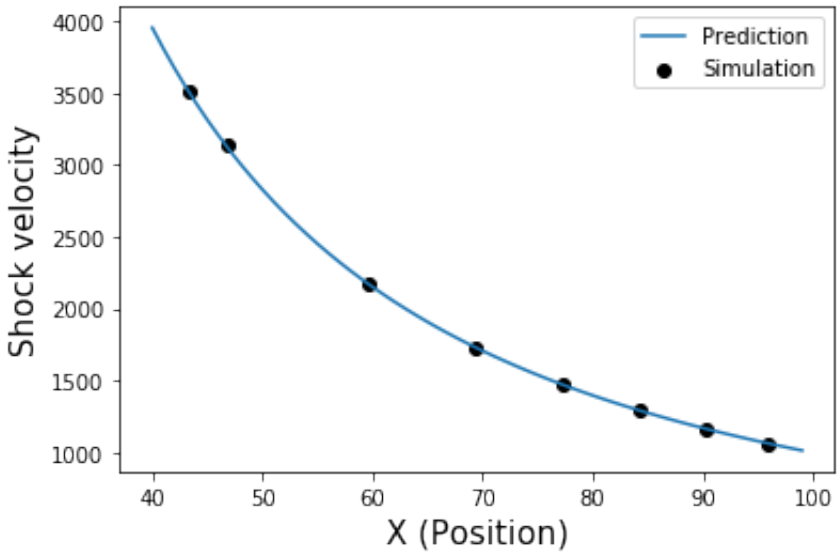

Figure 6: A plot of shock velocity vs. shock position from our numerical simulation over-plotted with the analytical solution that $v \propto R^{-3/2}$. For the model to fit, we used a coefficient of 989938.36 in front of the $R^{-3/2}$.

From this figure it is clear that the values obtained from the simulation for D vs. R_{shock} are in agreement with the analytical solution.

4.4 Pressure vs. Time

Here we answer question 4 in P.121.

For question 4, we would first derive the semi-analytical solution. From Landau's derivation, we first utilize jump conditions to get equations that relate pressure in the post-shock region to values in pre-shock region and shock velocity [1]:

$$P_1 = \frac{2}{\gamma + 1} \rho_0 D^2 \tag{21}$$

where ρ_0 is the density in the pre-shock region, and D is the shock velocity [2]. P_1 is the pressure in the post-shock region relative to a fixed coordinate system [2].

Then, we would combine equation 4 to get the pressure directly related to time. However, in order to expand equation 4, we still need to know the equation for R(t):

$$R(t) = \beta\left(\frac{Et^2}{\rho_0}\right)^{\frac{1}{5}} \tag{22}$$

where β can be derived by solving the integral that gives us total energy:

$$E = \int_0^R \rho[\frac{1}{2}v^2 + c^2/\gamma(\gamma-1)]4\pi r^2 dr \tag{23}$$

In terms of similarity variables, equation 23 can be expressed as:

$$\beta^5 \frac{16\pi}{25} \int_0^1 \psi[\frac{1}{2}\phi^2 + f/\gamma(\gamma-1)]\eta^4 d\eta = 1 \tag{24}$$

By plugging in the condition for $\gamma = 1.4$, we get $\beta = 1.033$ [2].

Therefore, we can combine equation 4, 21, and 22 to get the pressure vs. time equation:

$$P = \frac{2}{\gamma+1}\rho_0 \left[\frac{2}{5}\beta\left(\frac{E}{\rho_0}\right)^{1/5} t^{-3/5}\right]^2 \tag{25}$$

Therefore, by plugging in the initial conditions and β value, we can get a coefficient to be 0.00621.

For the numerical solution, we choose the fixed point r = 61.43, and thus we need to find the analytical value for the time that shock front passes this point. By using equation 22, we work out the time t = 0.012. Then, we can find the pressure vs. Δt relation.

The semi-analytical solution is over-plotted with numerical solution on Figure 7.

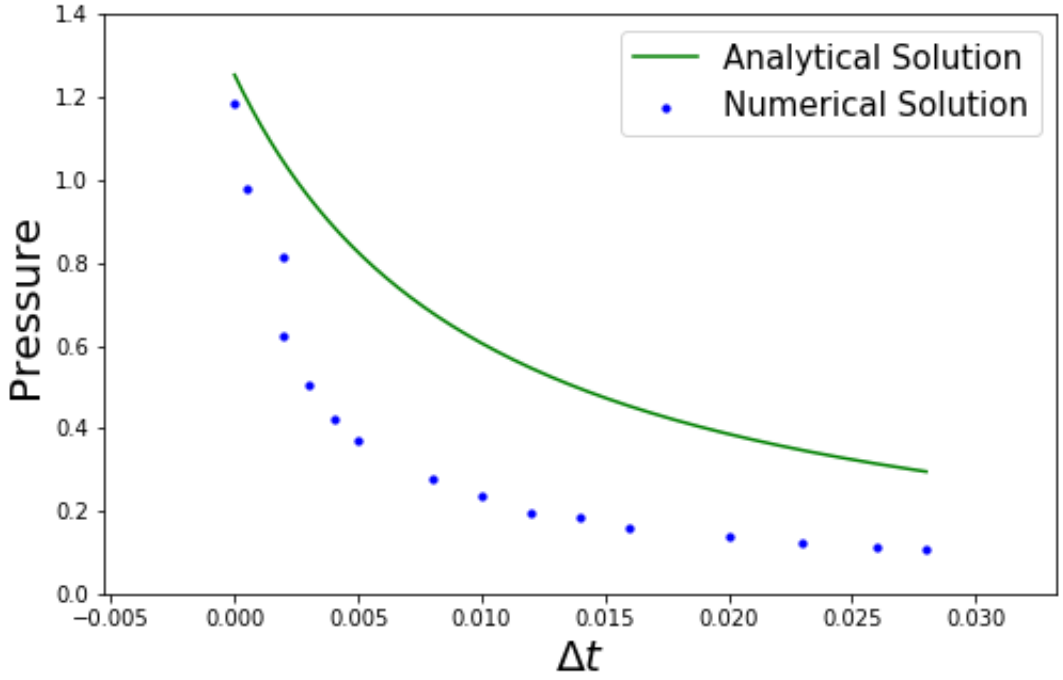

Figure 7: Comparison between numerical solution and semi-analytical solution for pressure vs. time at a fixed point (r = 61.43) after the wave front passes this point.

From the plot, we discover that the analytical solution returns a slightly larger value comparing to the numerical solution.

4.5 Glitches

The idea of the similarity variables is that even though the blast wave propagates with time, the shape and behavior of f, ϕ, and ψ are unchanged. Previously, when we let the shock front propagate to R = 100, the wave is pretty stable and all three plots from numerical solutions are well lined up with analytical solutions. However, if we let the wave to just propagate through a few grids, for example R = 15.68, t = 0.0004, then we can see the curves from numerical solutions aren't lined up very well with semi-analytical solutions (Figure 8).

From plots of f, ϕ, ψ vs. η separately, we can further see the difference between numerical and semi-analytical solution (Figure 9-11).

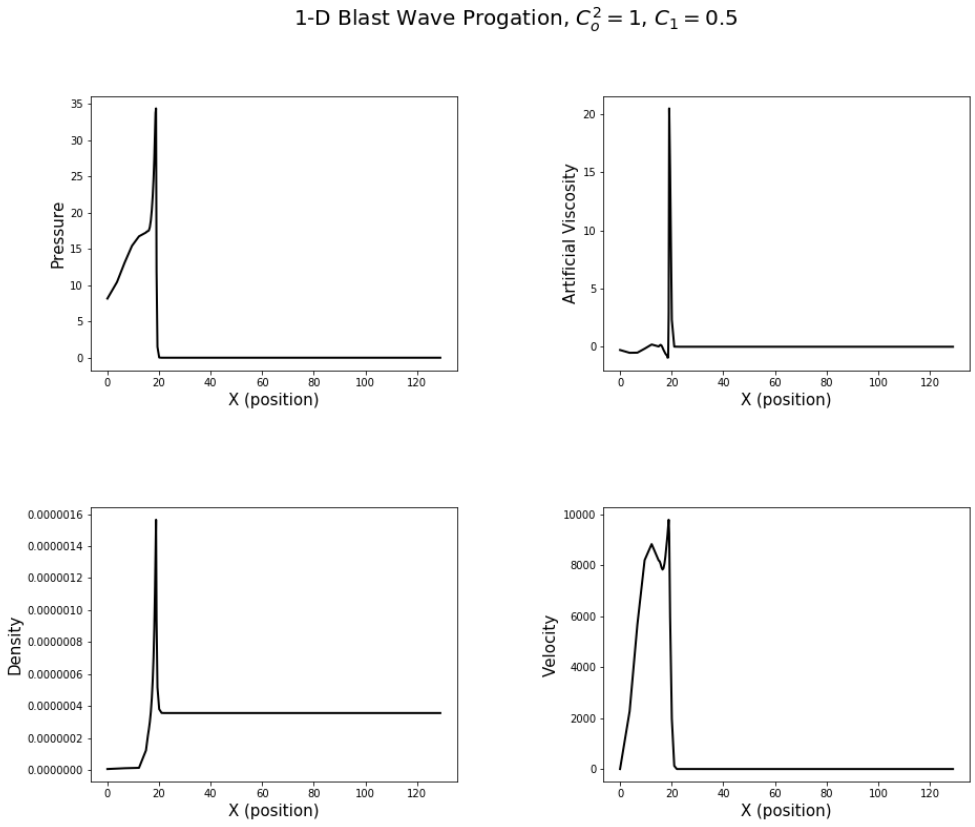

Figure 8: Blast wave propagation for $C_0^2 = 1$ and $C_1 = 0.5$, when R = 15.68, t = 0.0004. Four plots are pressure, artificial viscosity, density, and velocity versus coordinate position respectively.

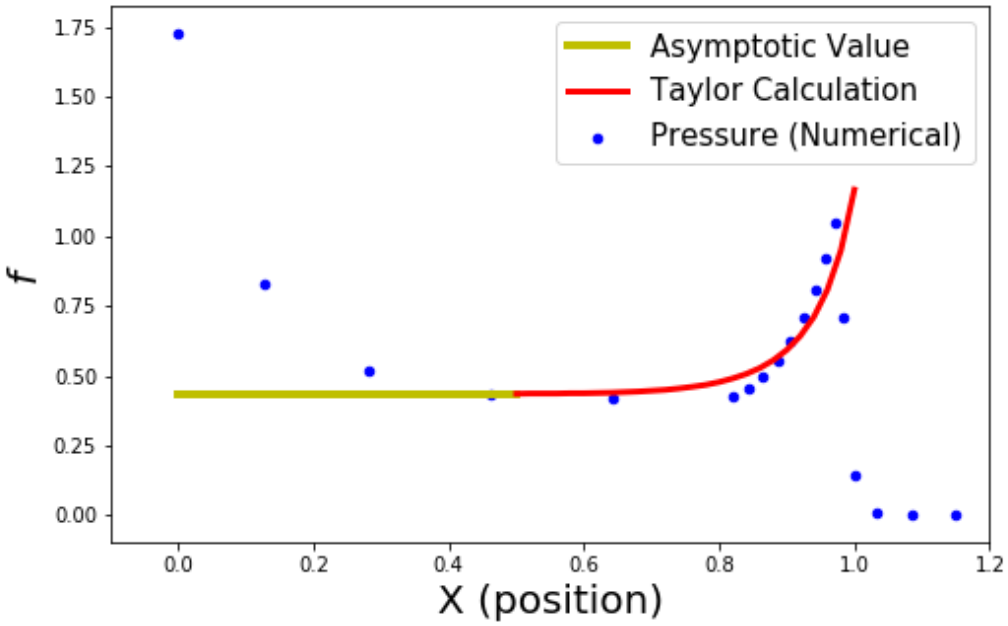

Figure 9: Comparison between numerically-calculated f and Taylor's result. Yellow curve shows the asymptotic value f as η approaches 0. Red curve shows Taylor's step-by-step calculation result.

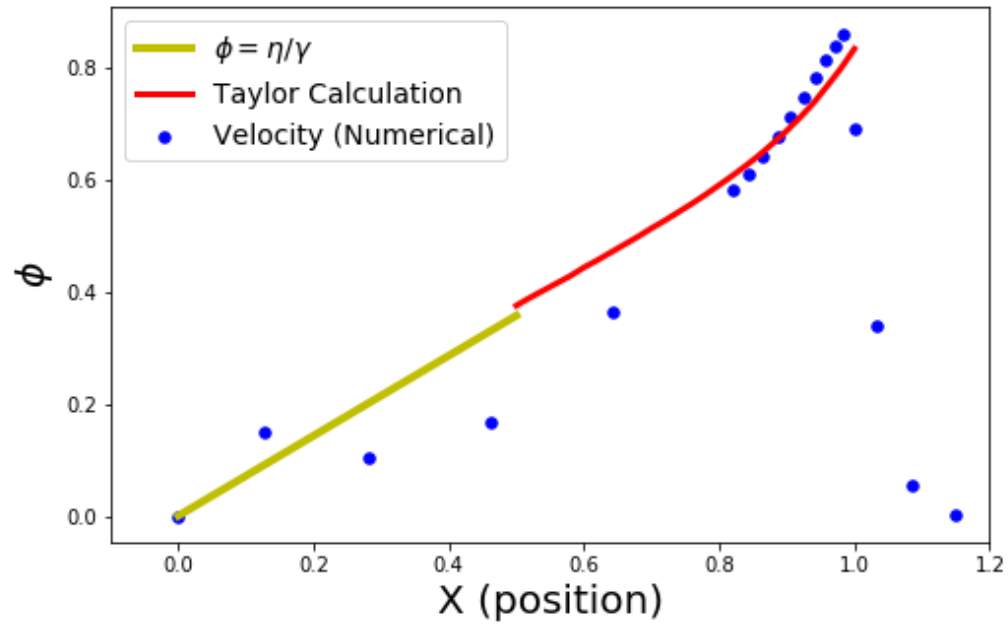

Figure 10: Comparison between numerically-calculated ϕ and Taylor's result. Yellow curve shows the linear trend of ϕ as η approaches 0. Red curve shows Taylor's step-by-step calculation result.

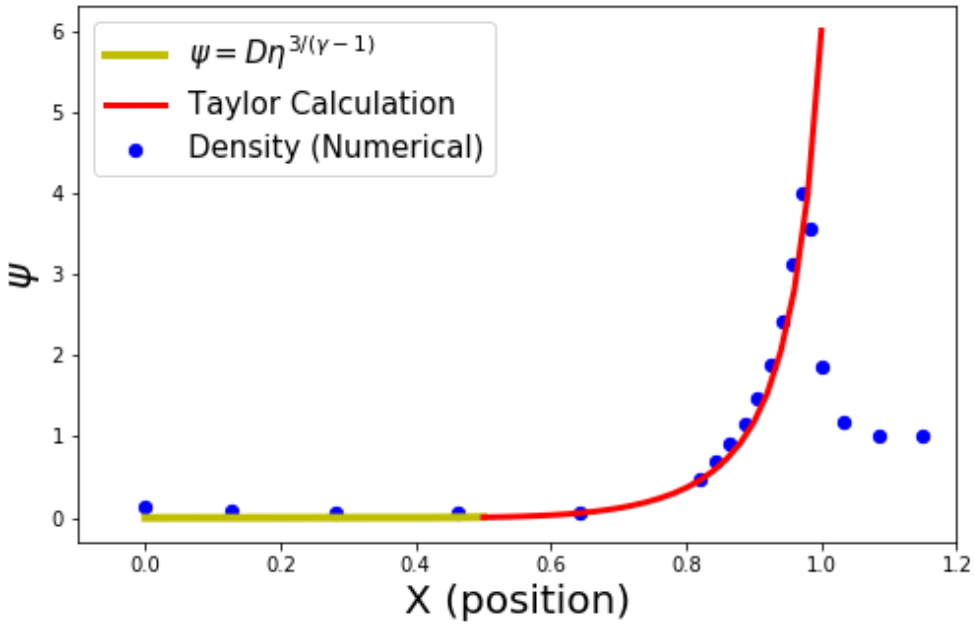

Figure 11: Comparison between numerically-calculated ψ and Taylor's result. Yellow curve shows the approximate formula result of ψ as η approaches 0. Red curve shows Taylor's step-by-step calculation result.

We can see that the largest deviation comes from f vs. η plot. This glitch effect comes from the fact that the Sedov Blast Wave semi-analytical solutions are based on the assumption that $M_{sw} >> M_0$ (the mass that the blast wave swept up is much larger than the initial explosion mass). At the start of the propagation, the mass and energy in the explosion zone is really large, and thus the mass swept up by it is not sufficient to slow down the shock. Therefore, at first, $R \propto Dt$, and only when the mass swept by the blast wave is much larger than initial explosion mass, the velocity of shock would decrease due to collisions with medium particles, and $R \propto t^{2/5}$. However, numerical equations are the same for all periods, so at first, there's a difference between these two solutions.

4.6 R(t) vs. Time

Since we already derive D vs. R plot (Figure 6) that's similar to deriving D vs. time plot, and we also derive pressure vs. Δt plot (Figure 7). Therefore, here we only focus on comparing the numerical solution to semi-analytical

solution of R(t) vs. time (Figure 12).

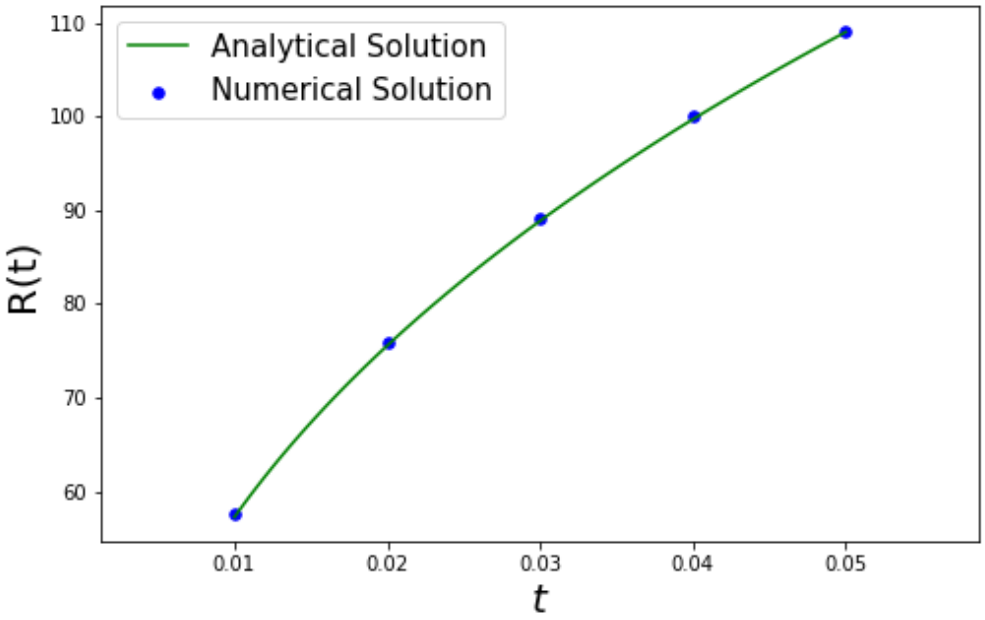

Figure 12: R(t) vs. time plot from numerical and semi-analytical solution

From this figure it is clear that the two solutions are lined up pretty well.

References

[1] L.D. LANDAU and E.M. LIFSHITZ. "CHAPTER IX - SHOCK WAVES". In: *Fluid Mechanics (Second Edition)*. Ed. by L.D. LANDAU and E.M. LIFSHITZ. Second Edition. Pergamon, 1987, pp. 313–360. ISBN: 978-0-08-033933-7. DOI: https://doi.org/10.1016/B978-0-08-033933-7.50017-9. URL: http://www.sciencedirect.com/science/article/pii/B9780080339337500179.

[2] L.D. LANDAU and E.M. LIFSHITZ. "CHAPTER X - ONE-DIMENSIONAL GAS FLOW". In: *Fluid Mechanics (Second Edition)*. Ed. by L.D. LANDAU and E.M. LIFSHITZ. Second Edition. Pergamon, 1987, pp. 361–413. ISBN: 978-0-08-033933-7. DOI: https://doi.org/10.1016/B978-0-08-033933-7.50018-0. URL: http://www.sciencedirect.com/science/article/pii/B9780080339337500180.

[3] Geoffrey Taylor. "The Formation of a Blast Wave by a Very Intense Explosion. I. Theoretical Discussion". In: *Proceedings of the Royal Society of London Series A* 201.1065 (Mar. 1950), pp. 159–174. DOI: 10.1098/rspa.1950.0049.